Contents lists available at **SCCE**

Journal of Soft Computing in Civil Engineering

Journal homepage: www.jsoftcivil.com

An Innovative Optimized Design for Laminated Composites in terms of a Proposed Bi-Objective Technique

F. Javidrad[1*], M. Nazari[2], H.R. Javidrad[3]

1. Professor, Department of Mechanical and Aerospace Engineering, Aeronautical University of Science and Technology, Tehran, Iran
2. Graduate Student, Center for Postgraduate Studies, Aeronautical University of Science and Technology, Tehran, Iran
3. Ph.D. Student, Department of Mechanical Engineering, University of Manitoba, Winnipeg, Canada

Corresponding author: *f.javidrad@gmail.com*

https://doi.org/10.22115/SCCE.2020.218142.1173

ARTICLE INFO

Article history:
Received: 05 February 2020
Revised: 23 February 2020
Accepted: 23 February 2020

Keywords:
Laminated composites,
Layup design,
Bi-objective optimization,
Hybrid PSO-SA optimization,
Layup blending.

ABSTRACT

The article proposes a bi-objective optimization approach for layup design of laminates. The optimization method combines the Particle Swarm Optimization (PSO) heuristics and Simulated Annealing (SA) optimization method. The minimum weight optimization is subjected to design constraints such as strength, stiffness, layup blending continuity, and several manufacturing design rules, which are combined as a single function and included within the bi-objective formulation. Several composite materials design problems are included to show the capabilities and usefulness of the proposed method. The optimization analysis has also been connected to the finite element analysis to solve the problem of composite plate optimization with blending constraints. The plate is divided into some regions, and the blending constraints are imposed globally by using the concepts of the greater-than-or-equal-to blending to achieve continuity of laminate layups across the regions. The results generally showed that the proposed method led to excellent results, representing a promising approach for the design of laminated composite materials.

How to cite this article: Javidrad, F, Nazari, M, Javidrad HR. An innovative optimized design for laminated composites in terms of a proposed bi-objective technique. J Soft Comput Civ Eng 2020;4(1):01–28. https://doi.org/10.22115/scce.2020.218142.1173.

1. Introduction

Composite materials are part of the advanced materials with growing applications in many engineering fields. These materials have specific functions, and their directional properties enable to tailor them for a specific application. Complex mechanical behavior associated with a large number of variables causes the structural design of composite materials much more difficult and laborious than the structures made of isotropic (metallic) materials. These characteristics have encouraged the use of mathematical optimization methods in determination of the optimum shape and layup stacking sequence of the structure in a more sophisticated way to attain the maximum material efficiency and performance. Efficiency and performance of composite materials are in close relationship with design methodologies to define lamina thickness and orientation, resin and fiber materials, manufacturing, etc. to achieve reliability and resonable strength-to-weight and stiffness-to-weight ratios [1].

Research on the subject of composite materials optimization has been reported extensively. Generally, research in the field of optimum composite design focuses on the three areas of modeling, analysis, and optimization method, each of which is reviewed briefly.

● Modeling

The first step in the design optimization of laminated composites is the choice of material behavior modeling. Undoubtedly, the simplest way to optimize composites is when material behavior is expressed by closed-form mathematical relationships. If a closed-form solution exists, cost function computation and the sensitivity analysis will be managed efficiently. Since closed-form solutions are only available in simple cases and they generally involve many assumptions, this approach is normally conducted in the design of laminates at the material level. Employing the Classical Lamination Theory (CLT), effective stiffness parameters, stresses, critical buckling loads, and some other physical characteristics of laminates can be expressed by closed-form equations. In material level optimization analysis, the thickness of lamina, fiber orientation, the volume percentage of fibers, and other parameters in lamina level are commonly considered as design variables. For the sake of simplicity and computational efficiency, much of the research in the field of composite optimization has focused on material-level design. Optimum weight design of laminates with given stiffness properties [2], maximizing buckling load-carrying capacity of laminated composite [3], optimum design of laminates against fatigue loads [4] are only a few examples from literature, in which closed-form solutions are used for optimization purposes. For more complicated models such as reinforced plates, plates with cutouts, structures with 3D fiber placement, curved shells and 3D structures numerical methods such as finite element method is currently used [5].

● Analysis

To date, several theories have been developed to determine kinematic behavior and stress distributions in composite laminates. Robbins & Reddy (1993) [6] categorized the analysis

methods based on the displacements or stress distributions through the laminate thickness to two classes: Equivalent Single Layer (ESL) and Layer-wise (LW) theories. The main difference of these methods is on the assumption of shear stress distribution in the thickness direction and transverse deformation of the laminate.

ESL-based theories, reduce a 3D problem to a 2D one by defining the displacement as a linear combination of pre-defined functions and mid-plane displacement components. ESL is further classified into CLT [7], First Order Shear Deformation (FSDT) [8], and Higher-order Shear Deformation (HSDT) theories [9].

Classical lamination theory ignores shear deformations through the thickness and involves only three variables. However, in FSDT, shear deformation in the thickness direction is estimated by a linear function and therefore, it involves five variables. The main drawback of FSDT is that the equilibrium equations are not satisfied in the upper and lower surfaces of the plate. To compensate for the difference between the linear assumed stress and the real stress distributions, a corrective coefficient is often necessary. This coefficient is a function of the stack sequence and cannot be defined uniquely. In contrast, HSDT uses non-linear functions such as cubic, trigonometric, or hyperbolic functions to describe shear deformation in the thickness direction of the laminate. HSDT satisfy equilibrium equations but contains more variables, and thus is more computationally expensive [10]. Although ESL may be adequate for analysis of most practical composite laminates design problems, they typically fail to describe accurately the 3D stress field at the ply level. This deficiency is primarily related to the assumption of continuous transverse strain components across the interface of the lamina, which causes discontinuity of the transverse stresses.

In LW theories, each layer is treated separately, and specific displacement field expansions or constraints are applied within each layer to yield a sort of continuity across the layer interfaces and a more accurate description of the complete stress state [11]. For instance, in a research work, each layer of a laminate was considered as an independent plate, and the compatibility of displacements at layer interfaces have been enforced by using the Legendre polynomials [12].

In the optimization process, different layups are examined iteratively, and hence, the calculation of the shear stress correction factor is crucial and costly. In this respect, for thin laminates, CLT is the easiest choice. However, for thick laminates, FSDT or other high order theories with an approximate shear stress correction factor, or finite element analysis should be used, even though it enforces much computational cost to the analysis.

- Optimization methods

Mathematical optimization methods, both deterministic and evolutionary stochastic search approaches, are widely used in the design of composite structures [13]. In the most design cases, the objective is the minimization of the total thickness or weight of the structure subjected to

constraints such as stiffness, strength, natural frequencies, critical buckling loads, and manufacturing requirements.

Deterministic methods usually require objective function to be continuous and differentiable. Moreover, these methods can readily converge to a local optimum points. However, the application of these methods in real large design problems involving discrete and/or integer variables is limited. On the other hand, stochastic random search optimization methods can handle combinations of continuous and non-continuous functions, and can approach to the global optimum solution. However, evolutionary search methods generally necessitate a large number of objective function evaluation for thorough exploration of the feasible region. Besides, an algorithm is always needed to prevent convergence to local optimum points [14].

For design optimization of composite laminates, stochastic search methods have been addressed broadly in the literature. Genetic Algorithm (GA) [15,16], Simulated Annealing (SA) [2,6], Ant Colony [17], Particle Swarm Optimization (PSO) [18,19] and hybrid methods such as PSO-SA [20] and PSO-GA [21] are among the methods that are referred to extensively.

In this article, a bi-objective optimization procedure based on the hybrid PSO-SA method is proposed for the design of laminated composites. The adopted hybrid PSO-SA optimization method is inspired from the method previously developed by Javidrad, & Nazari (2017) [22] and implemented to design of laminates by using penalty functions [20]. Stiffness, strength, layup blending continuity, and several design and manufacturing rules were incorporated into the formulation. Both CLT solutions and finite element modeling were used to compute the stiffness and strength properties of the laminate. Three design problems, including A_{22} stiffness parameter maximization, weight optimization of a laminate under in-plane forces and moments, and weight optimization of a plate under bending loads including layup blending constraint were presented.

2. Analysis of composite laminates

Consider a laminated composite plate as shown in Fig. 1(*a*), with reference plane $z = 0$ located at the mid-plane. Based on the Kirchhoff's hypothesis, the displacement components are

$$\begin{aligned} u &= u_0 + z\frac{\partial w}{\partial z}, \\ v &= v_0 + z\frac{\partial w}{\partial y} \\ w &= w_0 \end{aligned} \tag{1}$$

where *u*, *v* and *w* are small displacements along the *x*, *y* and *z* directions, respectively.

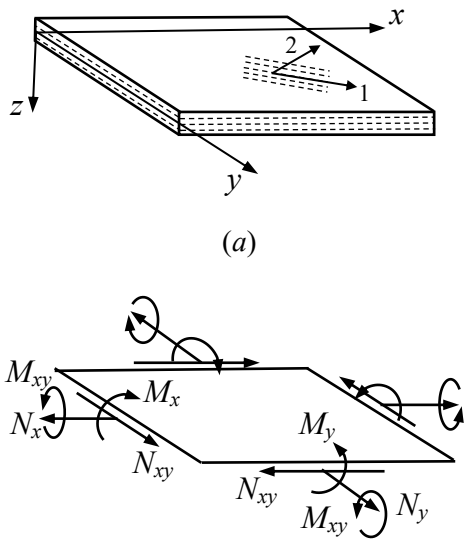

Fig. 1. (*a*) Geometry of a laminate with global (*xyz*) and material (1-2) coordinate systems. (*b*) Definition of force and moment resultants.

The forces and moments per unit length of the cross-section can be found by integrating stress components in the thickness direction. Eqs. 2 describes the in-plane stress resultant forces $[N_x, N_y, N_{xy}]^T$, and resultant bending moments $[M_x, M_y, M_{xy}]^T$.

$$\begin{bmatrix} N_x \\ N_y \\ N_{xy} \end{bmatrix} = \sum_{k=1}^{n} \int_{z_{k-1}}^{z_k} \begin{bmatrix} \sigma_x \\ \sigma_y \\ \sigma_{xy} \end{bmatrix} dz \tag{2a}$$

$$\begin{bmatrix} M_x \\ M_y \\ M_{xy} \end{bmatrix} = \sum_{k=1}^{n} \int_{k-1}^{k} \begin{bmatrix} \sigma_x \\ \sigma_y \\ \sigma_{xy} \end{bmatrix} z\, dz \tag{2b}$$

where σ_x, σ_y and σ_{xy} are two normal and shear stresses developed in lamina, respectively, and n represents the number of layers in the laminate. By implementing constitutive relations in global coordinates [23], the relationships between the resultant forces and resultant moments and the global mid-plane strains (ε) and curvatures (κ) can be derived as below:

$$\begin{aligned} [N] &= [A][\varepsilon] + [B][\kappa] \\ [M] &= [B][\varepsilon] + [D][\kappa] \end{aligned} \tag{3}$$

where A, B and D are stiffness matrices. The components of these matrices are calculated as:

$$A_{ij} = \sum_{k=1}^{n} (\bar{Q}_{ij})_k (z_k - z_{k-1}) \quad i, j = 1, 2, 6 \tag{3a}$$

$$B_{ij} = \frac{1}{2} \sum_{k=1}^{n} (\bar{Q}_{ij})_k (z_k^2 - z_{k-1}^2) \quad i, j = 1, 2, 6 \tag{3b}$$

$$D_{ij} = \frac{1}{3} \sum_{k=1}^{n} (\bar{Q}_{ij})_k (z_k^3 - z_{k-1}^3) \quad i, j = 1, 2, 6 \tag{3c}$$

where $(\bar{Q}_{ij})_k$ denote components of the reduced stiffness matrix of the *k*th lamina in the global coordinate system. If the same materials is used for each lamina in a laminate, the stiffness matrices can also be expressed in invariant forms [23].

2.1. Stress-based failure analysis

In the design of laminated composite materials, a comprehensive strength-based failure criterion is required. The failure criterion must be able to predict the failure of a laminate for any layup configuration. However, due to the interaction between the layers, accurate failure prediction of a laminated composite materials is rather complicated [24].

To date, several strength-based failure criteria have been suggested. Limit-based theories (maximum stress or strain) [25], polynomial-based theories [26,27], strain energy-based theories (e.g. Tsai-Hill failure criterion)[28], and direct mode determining theories [29,30] are among those that extensively used in practice. Rohwer (2015) [31] presented a review of the failure criteria for fiber composite materials.

In this study, failure is determined by the "first ply failure" (FPF) approach following the maximum stress (MS) and Tsai-Wu (TW) ply-level failure criteria. In many references (e.g. [32]) certain combinations of failure theories have been suggested for actual failure analysis to limit shortcomings of each failure criterion.

A micromechanical study [33] showed that for a lamina with fiber orientation angles between 0° and 30° the TW criterion is accurate enough, while for fiber orientation angles between 60° and 90° the MS criterion can suitably predict the failure. However, for fiber orientation angles between 30° and 60°, a linear combination of the two failure criteria may be adopted as described by Eq. 4[20].

$$(IF)_{mixed} = \alpha_1 (IF)_{MS} + \alpha_2 (IF)_{TW} \tag{4}$$

Where $(IF)_{mixed}$ denotes the mixed index factor. The index factor is the ratio of the stresses to strength in which the values of greater than 1 represent failure. α_1 and α_2 are the linear combination constants, which can be typically set to 0.9 and 0.1, respectively [20] . $(IF)_{MS}$ and $(IF)_{TW}$ denote respectively index factors associated with the MS and TW failure criteria defined as:

$$(IF)_{MS} = \max\left(\left(\frac{\sigma_1}{X_t} or \frac{\sigma_1}{|X_c|}\right), \left(\frac{\sigma_2}{Y_t} or \frac{\sigma_2}{|Y_c|}\right), \frac{\sigma_{12}}{S}\right) \tag{5}$$

$$(IF)_{TW} = F_1\sigma_1 + F_2\sigma_2 + F_{11}\sigma_1^2 + F_{22}\sigma_2^2 + F_{66}\sigma_{12}^2 \tag{6}$$

$$\begin{aligned} &F_1 = \frac{1}{X_t} - \frac{1}{|X_c|}, \quad F_2 = \frac{1}{Y_t} - \frac{1}{|Y_c|}, \\ &F_{11} = \frac{1}{X_t|X_c|}, \quad F_{22} = \frac{1}{Y_t|Y_c|}, \\ &F_{66} = \frac{1}{S^2} \end{aligned} \tag{7}$$

where X_t, X_c, Y_t and Y_c denote the ultimate tensile and compressive strengths in the fiber and the transverse directions, respectively. S denotes the in-plane shear strength of the lamina. σ_1, σ_2, and σ_{12} are two lamina normal and shear stresses in material coordinates.

2.2. Composite laminate design for manufacturing guidelines

Several guidelines have been established based on previous experience from design, test, and manufacturing to support the designer utilizing best the composite material strength. The purpose of these guidelines is to avoid the occurrence of critical failure modes and simultaneously guarantee a manufacturable design. These guidelines are usually defined on the ply level in thickness or the longitudinal direction. Bailie et al. (1997) [34] and Kin et al. (2005) [35] suggested several rules for stacking sequence design. Some of these design rules are described below:

(1) Symmetry: In most of the real applications, the stack of a laminate are selected to be symmetric about its mid-plane to make the design analysis simple. Symmetry also offers simplicity in testing, the description of allowable properties, and manufacturing. In symmetric laminates components of membrane/bending matrix, as defined in Eq. (3b), are zero. Vannucci and Verchery (2001)[36] discussed a more general state for uncoupling of membrane/bending deformations in laminated composites.

(2) Balancing: A balanced layup represents uncoupling in in-plane normal and shear responses. Moreover, balancing condition decreases the values of bending-twisting coupling terms in D matrix resulted in a simpler bending response of the laminate (see Eq. 3). Montemurro (2015) [37] discussed the conditions of a fully orthotropic laminate and uncoupled membrane and bending responses.

(3) 10% rule: A practical laminate should have a minimum 10% of layers should have fiber orientations 0°, ±45°, and 90° [34] . This choice makes the laminate fiber dominated, and provide good damage tolerance and durability [38].

(4) Contiguity constraint: The thickness of a lamina is directly related to the interlaminar stress, which affects the occurrence of free edge delamination. This design rule concerns a limitation to the thickness of adjacent plies with the same fiber orientation angle. According to Niu (2010) [39], for a laminate with a standard ply thickness (0.127 *mm*), not more than four contiguous plies should be used.

(5) Separation of $\pm\theta$ layers: Separation of layers with $\pm\theta$ fiber orientations can lessen interlaminar shear stresses and therefore gives more delamination strength to the laminate [35] .

(6) Disorientation constraint: when the relative fiber orientation angles difference between two successive layer is greater than a limit value, significant interlaminar stresses will be developed, which can promote failure. To postpone matrix cracking and the occurrence of delamination, it is better to use 45° as a limit for the ply angle difference between two adjacent plies [40].

3. Optimization method

Particle swarm optimization (PSO) is a population-based random search technique motivated by the intelligent social behavior of animals. [41]. This method is first proposed by Kennedy and Eberhart (1995) [42]. The main idea behind the PSO algorithm is using a swarm to simultaneously search a large region in the feasible space coupled with artificial life characteristics.

Consider a set of particles that are distributed uniformly across an *n*-dimensional search space. In each PSO iteration, the position of the particle *k* is updated by the addition of the vector v_k, called velocity, to the previous position vector (Eq. 8). The velocity vector is calculated according to Eq. (9), in which two vectors representing the difference between the current and the best position of the particle, and the current and the global best position of the particle are incorporated.

$$X_k^{i+1} = X_k^i + v_k^{i+1} \tag{8}$$

$$v_k^{i+1} = \omega v_k^i + c_1 R_1 (P_k^b - X_k^i) + c_2 R_2 (P^g - X_k^i) \tag{9}$$

where $X_k^i = [X_1^i, X_2^i, \cdots, X_n^i]^T$, $P_k^b = [P_1^b, P_2^b, \cdots, P_n^b]^T$, and $P^g = [P_1^g, P_2^g, \cdots, P_n^g]^T$ denote the state of particle *k* at iteration *i,* the best state of particle *k* in the search space, and the global best position reached by all particles, $P^g = [P_1^g, P_2^g, \cdots, P_n^g]^T$, respectively. R_1 and R_2 are two random numbers that vary between 0 and 1, and c_1 and c_2 are cognitive and social parameters which are problem-dependent constants. In fact, c_1 and c_2 control the magnitudes of particle velocity, and hence its movement, along the directions of a particle best position and the global best position of the swarm. A limit velocity, v_{max}, is usually defined to prevent particles from moving off the search space. Accordingly, the velocities are bounded as:

$$v_k^{i+1} = \begin{cases} v_{\max} & v_k^{i+1} \geq v_{\max} \\ -v_{\max} & v_k^{i+1} \leq -v_{\max} \end{cases} \tag{10}$$

ω is a multiplier, known as the inertia factor, used to further control the velocity by making a balance between exploration and exploitation. Exploration and exploitation are referred to as the ability of a particle movement across the entire search space and inside a local region, respectively. The balance between exploration and exploitation is important to approach the global optimum point by facilitating jumping out of the local optimum points. Although there are many suggestions for this function, a linear step function defined as Eq. 11 is usually used [43].

$$\omega = \omega_{\max} - \left(\frac{\omega_{\max} - \omega_{\min}}{i_{\max}} \right) \times i \tag{11}$$

where i_{max} is the maximum allowable solution iteration number. ω_{max} and ω_{min} are two limit values of ω.

The main shortcoming of the PSO algorithm is that it may trap into a local optimum if an improper balancing between exploration and exploitation is provided. Javidrad and Nazari (2017) [22] suggested a hybrid method to improve the social performance of a swarm by a systematic updating the global best position of the swarm. In this respect, when no further improvement in the global best position recognized in a PSO cycle, the SA algorithm is implemented to improve the global best position of the swarm.

SA is a global optimization method based on the Metropolis Monte Carlo procedure. SA uses the Metropolis method to accept a state probabilistically with higher function value. The acceptance probability is defined as

$$P = \begin{cases} 1 & f(X_{i+1}) \le f(X_i) \\ \exp(-\Delta f / T) & Otherwise \end{cases} \tag{12}$$

Where Δf is the variation of the function between two successive points, and T is the acceptance parameter called temperature. Temperature controls the exploitation capability of the SA algorithm by limiting the acceptance probability. In fact, by sequentially decreasing *T,* the exploitation ability of the SA is promoted [44]. There are many temperature change functions, such as linear, logarithmic, and exponential functions [45]. The most widely used temperature decrement rule is:

$$T_{i+1} = R_T . T_i \tag{13}$$

where R_T is a positive decrement constant between 0.8 and 1.

Referring to the literature, there are a few algorithms developed based on the combination of PSO and SA. Xia and Wu (2006)[46] introduced a hybrid PSO-SA method in which PSO generates an initial candidate point for the SA analysis. In another approach (Wang & Li, 2004)[47], the position of each particle within the PSO optimization process is improved by the SA process. The integration of the Metropolis acceptance criterion with the PSO is another hybrid PSO-SA method, which has been suggested by Shieh et al. (2011) [48]. A more

comprehensive literature review on the subject of the hybrid PSO-SA optimization method has been given in Javidrad and Nazari (2017) [22].

The proposed hybrid algorithm essentially integrates good local search capability of the SA optimization method within the PSO. Fig. 2 shows the overall concept of this optimization method.

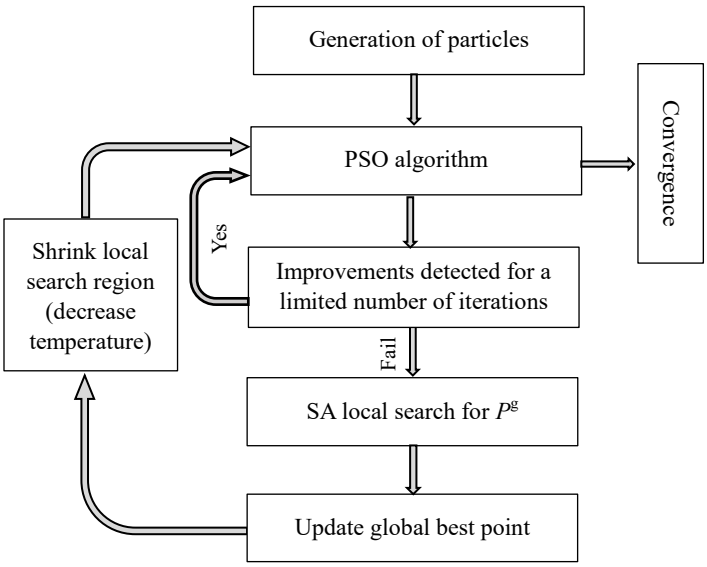

Fig. 2. Conceptual model of the hybrid optimization method.

This algorithm has been implemented and applied to unconstrained single objective optimization of several mathematical functions with various dimensions by Javidrad and Nazari (2017) [22]. It is reported that including SA within the PSO, upgrade stability and convergence rate of the solution process.

In the present study, however, a modified SA is implemented within the PSO-SA hybrid method. In this modified version of SA, the temperature change is adaptively related to the function decrease which cause the inner loop of the SA is ignored [49]. It is noted that the inner loop of the SA algorithm is related to the length of the Markov chain representing temperature stability within each SA loop.

4. Optimization problem description

The optimization problem concerns the design of a minimum weight laminate under the stiffness and strength constraints and to satisfy conventional design rules.

The optimization problem is formulated as a bi-objective problem as follows:

$$min\,(W, f) \tag{14}$$

where

$$W = \rho A \sum_{i=1}^{NoL} l_i t_i \tag{15}$$

$$f = \max(0, g_j(X_i)) \quad j = 1,2,3 \quad i = 1,2,\cdots,n \tag{16}$$

$$g_1(X_i) = \sum_{m=1}^{MP} \left(\frac{Sp_m^c - Sp_m^r}{Sp_m^r} \right)^2 - \varepsilon \le 0 \quad i = 1,2,\cdots,n \tag{17}$$

$$g_2(X_i) = \frac{\max(IF_{mixed})_i}{(IF)_{all}} - 1 \le 0, \quad i = 1,2,\cdots,n \tag{18}$$

$$g_3(X_i) = \sum_{k=1}^{MC} h_k(X_i) \le 0, \quad i = 1,2,\cdots,n \tag{19}$$

where n and NoL denote the number of laminae and number of the local regions, respectively. ρ, t, A, Sp^c, Sp^r, MP and, ε are the density, lamina thickness, panel area, the required and calculated stiffness parameters, the number of stiffness parameters to be included in the analysis and the stiffness tolerance value, respectively. $(IF_{mixed})_i$ denotes the index factor determined for the ith lamina, and $(IF)_{all}$ is the allowable index factor. Similar to the factor of safety, the choice of the allowable index factor is dependent on the design and specific application. To provide an adequate margin of safety, in this work, the value of 0.83 has been chosen for the allowable index factor. This value gives a factor of safety of 1.2 to the failure of layers. MC is the number of design rules to be included in the design process, and X_i is the vector of design variables. It is noted that for a single lamina, three variables (t, θ, l) are incorporated into the optimization formulation. The first two are lamina thickness and orientation angle, which are continuous or discrete variables, and the third one is an integer contiguity variable that determines how many panels a lamina extended. The contiguity variable can be greater than one only for problems concerning blended laminate layup.

$$\begin{aligned} &X_i = (t, \theta, l)_i, \qquad i = 1,\cdots,n \\ &-90^\circ \le \theta \le 90^\circ \\ &t_l \le t \le t_u \\ &1 \le l \le N_{Reg} \end{aligned} \tag{20}$$

Where t_l, t_u, and N_{Reg} are the lower and upper limits of lamina thickness, and the number of regions in the laminate, respectively. h_k is an integer function introduced to characterize the degree of the manufacturing constraints violation. h_k varies between 0 for all constraints violated, and 5 for all constraints satisfied. The symmetry condition is always enforced in this analysis and thus is not included in h_k.

$$h_k = \begin{cases} 0 & \text{if } k\text{th constraint is satisfied} \\ 1 & \text{if } k\text{th constraint is not satisfied} \end{cases} \tag{21}$$

5. Implementation

● Initial swarm is generated and distributed uniformly across the design space (i.e., within the lower and upper bound of the design variables). For all case studies discussed in this article, the population size was 50.

● The parameters of the optimization analysis have been selected as in Table 1. It has been shown that these are optimized parameters for a range of mathematical and engineering problems [22]. These parameters remained constant in all case studies presented herein.

Table 1
The Optimized parameters of the proposed hybrid PSO-SA method.

T_0	R_T	ω_{max}	ω_{min}	c_1	c_2
1.0	0.95	0.55	0.1	0.8	1.7

● For each particle, the best position (P^b) at iteration i are determined. Similarly, the global best position (P^g) of the swarm is calculated. In the determination of these two positions, the following selection criteria are implemented:

(1) If the value of f is zero for two particles, the particle with the lower W value is selected.

(2) If the value of f is zero for one particle and nonzero for another, the particle with zero f is selected.

(3) If the value of f is not zero for two particles, the particle with the lower f value is selected.

At each iteration, every P^g with zero value of violence function f can be a potential optimum solution, i.e., Pareto solution. These solutions are stored for the final selection process.

● The velocity and position of each particle are updated according to Eq. (8) and Eq. (9). The new swarm is designated by X^{i+1}.

● The procedure continues until no improvement found in the global best solution during a PSO cycle. Then the method shifts to the SA, and the solution procedure continues for P^g. The SA loop length is pre-defined, and the final P^g determined during this loop returns to the PSO. The SA method used here is a modified one in which temperature is only updated when a move is accepted. By using this modified SA method, only one loop is necessary.

● The following convergence criteria have been used to terminate the solution procedure:

(1) The number of iterations reaches the prescribed maximum value.

(2) The temperature reaches to a tolerance value (namely, 10^{-3}).

● When the solution process terminates, the point with minimum W is selected from the solution vector as the final optimum solution.

6. Numerical results

6.1. Design of a laminate with maximum A_{22} stiffness coefficient

In this example, we seek ply stacking sequence of a laminate with n continuous plies that maximize A_{22} coefficient for a graphite-epoxy laminate. The composite is assumed to be symmetric and balanced. This problem, which is a variation of a composite design problem undertaken by Grosset et al. (2005) [50], has been approached by Venter and Haftka (2010) [51]. A constraint on the effective Poisson's ratio (ν_{eff}) and limitations in fiber orientation angles and ply thicknesses have been considered. The optimization problem can be stated as

$$\begin{aligned} &\textit{Maximize} && A_{22} = h(U_1 - U_2 V_1^* + U_3 V_3^*) \\ &\textit{Subjected to} && 0.48 \le \nu_{eff} \le 0.52 \\ & && -5^\circ \le \theta_k \le 5^\circ \quad \textit{or} \\ & && 40^\circ \le \theta_k \le 50^\circ \quad \textit{or} \\ & && 85^\circ \le \theta_k \le 95^\circ \\ & && 0.001 \le t_k \le 0.05 \end{aligned} \tag{22}$$

where

$$V_{\{1,3\}}^* = \frac{2}{h}\int_0^{h/2} \{\cos 2\theta, \cos 4\theta\}\, dz = \frac{2}{h}\sum_{k=1}^{n} t_k \{\cos 2\theta_k, \cos 4\theta_k\} \tag{23}$$

$$\nu_{eff} = \frac{A_{11}}{A_{22}} = \frac{U_4 - U_3 V_3^*}{U_1 - U_2 V_1^* + U_3 V_3^*} \tag{24}$$

and θ_k and t_k are ply angles and thicknesses (in inches), respectively. The U_i values are material invariants as given in Table 2.

Table 2
Invariant parameters of the graphite-epoxy composite.

Parameter	Value (psi)
U_1	0.8897×10^7
U_2	1.0254×10^7
U_3	0.2742×10^7
U_4	0.3103×10^7

Choosing n=3, we have only six design variables. This problem has been examined by a variety of methods such as single objective PSO algorithm using exterior quadratic penalty function and the adaptive penalty method, multi-objective PSO (MO-PSO), The modified multi-objective PSO using the crowding distance as the second selection criterion, and the PSO-SA algorithm presented herein. A maximum of 3000 function evaluations and a temperature limit of 10^{-8} were set as the termination criteria. To attain statistical results, several independent optimization runs were performed. The results are summarized in Table 3. The success rates, which is defined as the ratio of successful runs to the failed runs, are also given in Table 3. The successful runs are those reached to the known global solution.

The calculated layup stacking sequence by the proposed bi-objective PSO-SA method is very close to that of the other methods. When compared to the other multi-objective formulations as given in Table 3, the calculated maximum A_{22} is close enough to the global solution, 1.25×10^6 *psi* [51]. Typical variations of the A_{22} and ν_{eff} are shown in Fig. 3 and Fig. 4, respectively showing that the method explores the design space thoroughly and then stably approaches to the global optimum point.

Table 3
Optimization results for A_{22} maximization problem.

Parameter	Single objective PSO*		MO-PSO*	Modified MOPSO crowding*	PSO-SA (present wok)
	Quadratic penalty	Adaptive penalty			
Best layup orientation (degrees)	$[\pm95, \pm44.3, \pm44.5]_s$	$[\pm95, \pm44.3, \pm44.5]_s$	$[\pm95, \pm43.7, \pm42.3]_s$	$[\pm95, \pm44.8, \pm44.4]_s$	$[\pm95,\pm43.3, \pm44.4]_s$
Thickness (*in*)	$[0.0304, 0.05, 0.05]_s$	$[0.0304, 0.05, 0.05]_s$	$[0.0323, 0.05, 0.05]_s$	$[0.030, 0.05, 0.05]_s$	$[0.0312,0.05,0.05]_s$
ν_{eff}	0.4800	0.4800	0.4800	0.4800	0.4805
Success rate (%)	97	37	29	100	100
Maximum A_{22}	1.2505×10^6	1.2506×10^6	1.2434×10^6	1.2503×10^6	1.2485×10^6

* Taken from Venter and Haftka (2010) [51].

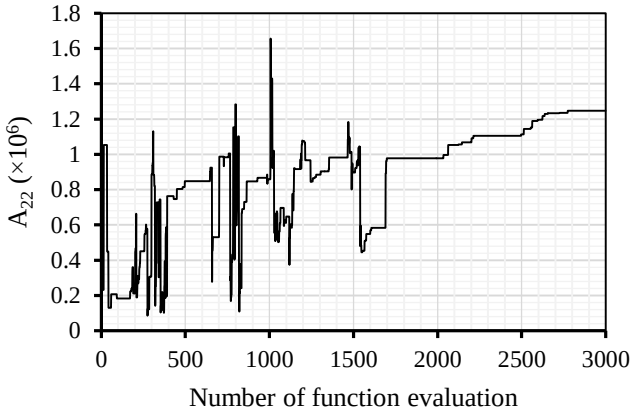

Fig. 3. Convergence behavior of A_{22} by the hybrid PSO-SA optimization method.

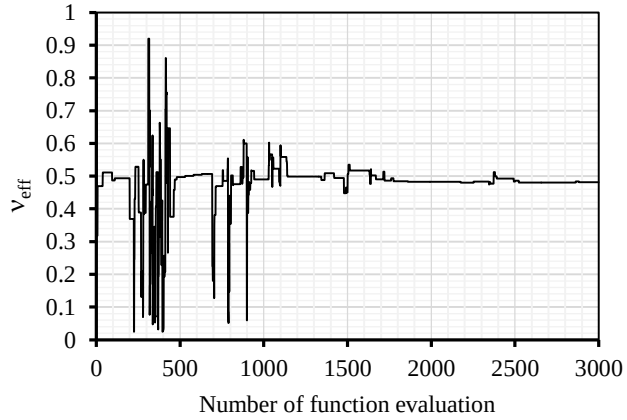

Fig 4. Convergence behavior of ν_{eff} by the hybrid PSO-SA optimization method.

As a continuation of the problem, we implemented discrete fiber angle orientation, layer thickness, and design rules as described in Section 2.2 to find a better design. It is assumed that the laminate comprises 32 layers with the layer thickness of 0.0083. This assumption gives a weight near to the previous results. The results for two fiber orientation angle steps (5° and 15°) are summarized in Table 4. The results given in Table 2 show that including more design rules to the optimization analysis will affect the maximum value determined for A_{22}. By reducing the design rules constraints, the maximum value of A_{22} can be greater than 1.25×10^6.

Table 4
Optimization results for A_{22} maximization problem including discrete variables and design rules constraints.

Angle	Case*	Layup	$A_{22}\times10^6$	ν_{eff}
5°	1	$[55,-50,-55,-50,45,-55,-65_2,-55,50,55,50,-45,55,65_2]_S$	1.385	0.4802
	2	$[65,-60,-50,55,45,55,-50,-60,-65,60,50,-55,-45,-55,50,60]_S$	1.385	0.4822
	3	$[-60,-55,-50,-60_2,-30,15,60_2,55,50,60_2,30,-15,-60]_S$	1.210	0.4809
	4	$[-55_2,-50,-40,0,45,50,90,55_2,50,40,0,-45,-50,-90]_S$	1.177	0.4809
15°	1	$[-60_2,45,-45,-60_2,60,-45,60_2,-45,45,60_2,-60,45]_S$	1.359	0.4886
	2	$[-60,-45_2,60,-60,-45,-60_2,60,45_2,-60,60,45,60_2]_S$	1.359	0.4886
	3	$[-45,-60,-45,-60_3,-45,0,45,60,45,60_3,45,0]_S$	1.171	0.5084
	4	$[-60,-45_3,0,45,90,45,60,45_3,0,-45,-90,-45]_S$	1.109	0.5165

*1: Including all design rules except the 10%, Contiguity and Disorientation design rules.
2: Including all design rules except the 10% and Disorientation rules.
3: Including all design rules except the 10% rule.
4: Including all six design rules.

6.2. Layup sequence design of a laminate under in-plane forces and moments

As the second design case study, a laminate made of Kevlar 49/epoxy with two different load cases has been considered. The laminate is assumed to be consist of twenty-ply groups. The optimization problem is to find the minimum laminate thickness based on design rules, to have the prescribed effective engineering coefficients and not to fail under the given set of loads.

To compare the results of this work with the published data, we set the material properties, load cases, and the prescribed engineering coefficients the same as those given by Javidrad et al. (2018a) [51] (see Tables 5-7). The Fiber orientation angle of each lamina was assumed to be multiples of 5°, 15°, and 45°. Two termination criteria were used: (*i*) the number of function evaluations exceeding 1×10^4 and (*ii*) the temperature approaching less than 1×10^{-8}.

Table 5
Typical elastic material constants of Kevlar 49/epoxy composite.

E_{11} (GPa)	E_{22} (GPa)	G_{12} (GPa)	ν_{12}	X_t (MPa)	X_c (MPa)	Y_t (MPa)	Y_c (MPa)	S (MPa)	ρ (kg/m^3)
76.0	5.5	2.3	0.34	1400	235	12	53	34	1450

Table 6
Loading conditions.

	Loading condition (1)	Loading condition (2)
N_x (N/m)	20000	2000
N_y (N/m)	130000	1400
N_{xy} (N/m)	0	0
M_x (N.m/m)	0	0
M_y (N.m/m)	0	150
M_{xy} (N.m/m)	0	0

Table 7
The required effective engineering constants.

E_{xx}^0 (GPa)	E_{yy}^0 (GPa)	G_{xy}^0 (GPa)	ν_{xy}^0	E_{xx}^f (GPa)	E_{yy}^f (GPa)	G_{xy}^f (GPa)	ν_{xy}^f
26.0	19	14	0.55	16	20	10	0.35

Superscript 0 and *f* stand for in-plane and flexural properties, respectively.

The best layup sequences found for each set of loads together with the results of the single-objective optimization process of Javidrad et al. (2018a) [51] are summarized in Table 8. The best layup sequences are those with zero function *f* (Eq. 16) and the least weight, which is selected from all potential optimum solutions. A comparison with this reference indicates better or similar results for all cases except case no. 6. In case no. 6, however, our index factor is lower than that given in the reference data. The effective engineering constants, as given in Table 9, show a minor difference with the required effective properties.

Table 8
The best calculated layup sequences.

Loading condition	Case	Stacking sequence	Fiber orientation angle step (Degree)	Weight (kg/m^2)	Index factor
(1)	1	$[45,90,45,40_3,0,-45,-90,-45,-40_3,0]_s$	5	5.278	0.824
	1*	$[45,90,45_2,35_3,0,-45,-90,-45_2,-35_3,0]_s$	5	6.032	0.683
	2	$[-45_2,-90,-45,-30_2,0,45_2,90,45,30_2,0]_s$	15	5.278	0.822
	2*	$[-45,-90,-45_4,-30_2,0,45,90,45_4,30_2,0]_s$	15	6.786	0.563
	3	$[-45_2,-90,-45_3,0_2,45_2,90,45_3,0_2]_s$	45	6.032	0.700
	3*	$[-45_2,-90,-45_3,0_2,45_2,90,45_3,0_2]_s$	45	6.032	0.700
(2)	4	$[-45_3,-90,-50,-25_2,0,45_3,90,50,25_2,0]_s$	5	6.032	0.741
	4*	$[45,90,45_4,25_2,0,-45,-90,-45_4,-25_2,0]_s$	5	6.786	0.690
	5	$[-45_3,-90,-45_2,-15,0,45_3,90,45_2,15,0]_s$	15	6.032	0.828
	5*	$[45_2,90,45_4,0_2,-45_2,-90,-45_4,0_2]_s$	15	6.786	0.633
	6	$[-45_2,-90,-45_4,0_2,45_2,90,45_4,0_2]_s$	45	6.786	0.622
	6*	$[45_2,90,45_3,0,-45_2,-90,-45_3,0]_s$	45	5.278	0.760

* represents the best results obtained from Javidrad et al. (2018a) [20].

Table 9
Effective engineering constants determined for each layup.

Case	E_{xx}^{0} (GPa)	E_{yy}^{0} (GPa)	G_{xy}^{0} (GPa)	υ_{xy}^{0}	E_{xx}^{f} (GPa)	E_{yy}^{f} (GPa)	G_{xy}^{f} (GPa)	υ_{xy}^{f}
1	24.130	20.090	14.291	0.533	15.476	22.634	9.960	0.306
2	28.248	20.062	13.291	0.523	17.267	20.823	10.078	0.338
3	28.470	21.181	12.984	0.491	18.440	20.562	10.653	0.351
4	28.145	20.178	13.292	0.520	17.251	19.118	10.347	0.369
5	26.814	20.669	13.520	0.511	16.719	18.805	10.642	0.382
6	26.473	20.232	13.698	0.524	17.239	19.687	10.719	0.370

6.3. Design of plate under bending loads and blending constraints

The optimum design of a composite plate with layup blending constraint is considered as the final example. In general, multi-region non-blended panel weight optimization with no continuity of laminate layup may be structurally non-profitable due to discontinuities. Although imposing the layup blending constraints gives rise to the complexity of the optimization process, it yields a more practical design. There are many approaches addressed in the literature for the design of composite laminates using layup blending concepts such as greater–than-or-equal-to blending [52] , sheared-layered blending [53], guide-based blending [54], and stacking sequence table based blending [55].

In the greater-than-or-equal-to blending method, a key panel is defined from which each ply emanates. The key panel is often the most loaded or the thickest region. Although each ply or lamina is allowed to be discontinued along the panel borders but once dropped, it is not allowed to be combined back into the other panels. Although this method is quite simple and can easily be implemented to the design process, it is not suitable for designing structures with several key panels.

To date, most of the works in composite structures design by layup blending methods have been centered on the single objective optimization using GA. In this example, however, we aimed at designing a cantilever composite plate using the concepts of the greater-than-or-equal-to blending by the proposed PSO-SA optimization in the framework of the bi-objective formulation. The plate is shown in Fig. 5, which is decomposed into three local panels.

As stated in Section 4, for a single lamina, three variables (t, θ, l) are incorporated into the optimization formulation. l is an integer contiguity variable that determines the extension of the lamina through the plate. In this example, we divided the plate into three equal panels, in which the Panel 1 is assumed to be the key region. In this respect, l=0 denotes that the lamina does not exist, l=1 designates the lamina only exists in the Panel 1, l=2 denote the lamina extended through the Panels 1 and 2, and finally, l=3 represents the lamina continues through all panels.

The design optimization problem is stated as a minimum weight design of the plate subjected to the maximum global deflection (in the Z-direction), first ply failure, local ply contiguity, and conventional design rules.

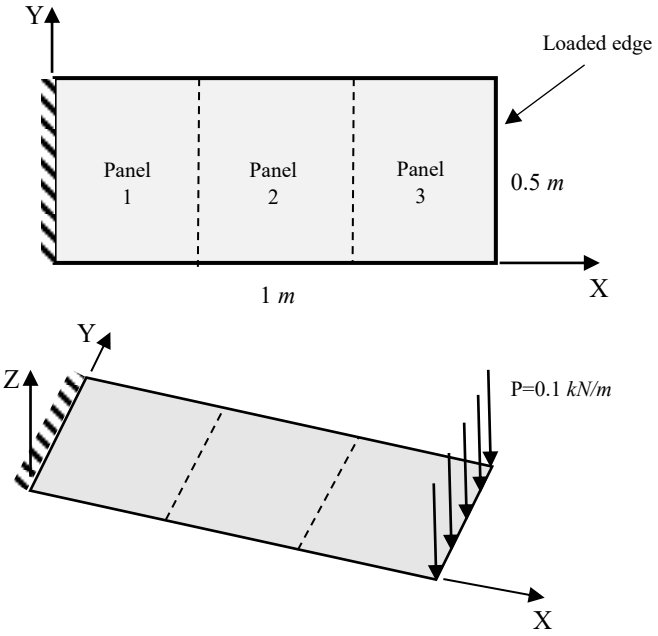

Fig. 5. Geometry of the cantilever composite plate.

In this example, the stiffness of the plate is represented by the global tip deflection in the Z-direction. In this regard, Eq. 17 is substituted by

$$\left| \left| \frac{w_{\max}}{\overline{w}} \right| - 1 \right| \leq 0.01 \tag{25}$$

where $w_{\max}$ and $\overline{w}$ denote the maximum calculated deflection in the z-direction and the maximum allowable deflection, respectively.

The in-plane material properties of the plate, which is made of carbon fiber epoxy laminate, are given in Table 10. The through-thickness material properties are assumed to be identical to those of the in-plane properties. A uniform distributed load of 0.1 *kN*/*m* is applied to the tip of the plate, as shown in Fig. 5.

Table 10
Typical elastic material properties of carbon/epoxy laminates.

E_{11} (GPa)	E_{22} (GPa)	G_{12} (GPa)	ν_{12}	X_t (MPa)	X_c (MPa)	Y_t (MPa)	Y_c (MPa)	S (MPa)	ρ (kg/m^3)
168	9.5	4.6	0.27	826	118	37	27	20	1600

A finite element uniform grid (25×15) consisting of 312 4-noded S4R composite shell element of ABAQUS software has been used to model the plate behavior. This shell element is well suited for moderate to thick composite plates since it accounts for transverse shear flexibility. The stress distribution through the thickness of each layer is determined by specifying several integration points through the thickness.

The optimization process has been linked to the finite element software to determine the maximum deflection and stresses as needed for the design optimization procedure. All parameters for the PSO-SA optimization analysis were set as given in Table 1. The maximum iteration was 9000. The results for $0.5 \le IF \le 0.83$ and $\bar{w} = 100\ mm$ are summarized in Table 11.

Table 11
The optimum blending layup sequences for all three panels.

Solution No.	panel	Stacking sequence	Index factor	Weight (kg)	Maximum Deflection (m)
1	1	$[-45_2,-15_2,-30,0_3,\ 45_2,15_2,30,0_3]_s$	0.592	7.6	0.1073
	2	$[-45_2,-15_2,0_3,45_2,15_2,0_3]_s$	0.564		
	3	$[-45_2,0_3\ ,45_2,0_2]_s$	0.513		
2	1	$[-45_2,-15_2,-25,0_3,45_2,15_2,25,0_3]_s$	0.591	7.6	0.106
	2	$[-45_2,-15_2,0_3,45_2\ ,15_2,0_3]_s$	0.553		
	3	$[-45_2,0_3,45_2,0_3]_s$	0.506		
3	1	$[-45_2,-15_2\ ,-30,0_3,45_2,15_2,30,0_3]_s$	0.592	8.0	0.0986
	2	$[-45_2,-15_2,-30,0_3,45_2,15_2,30,0_3]_s$	0.560		
	3	$[-45_2,0_3,45_2,0_3]_s$	0.511		
4	1	$[-45_2,-15_2,-45,0_3,45_2,15_2,\ 45,0_3]_s$	0.595	8.0	0.1009
	2	$[-45_2,-15_2,-45,0_3,45_2\ ,15_2,45,0_3]_s$	0.576		
	3	$[-45_2,0_3,45_2,0_3]_s$	0.519		
5	1	$[-45_3,-20,-5_3,0,45_3,20,5_3,0]_s$	0.514	8.4	0.101
	2	$[-45_3,-20,-5_3,0,45_3,20,5_3,0]_s$	0.564		
	3	$[-45_3,-20,0,45_3,20,0]_s$	0.518		
6	1	$[-45,-50,-15_2,-20_4,0,45,50,15_2,20_4,0]_s$	0.551	8.4	0.087
	2	$[-45,-15_2,-20_4,0,45,15_2,20_4,0]_s$	0.519		
	3	$[-45,-15_2,0,45,15_2,0]_s$	0.512		
7	1	$[-45_2,-15_2,-45_4,0,45_2,15_2,45_4,0]_s$	0.581	8.8	0.0986
	2	$[-45_2,-15_2,-45_4,0,45_2,15_2,45_4,0]_s$	0.666		
	3	$[-45,-15_2,0,45,15_2,0]_s$	0.600		
8	1	$[-45_3,-15,-35_4,0,45_3,15,35_4,0]_s$	0.510	9.2	0.107
	2	$[-45_3,-15,-35_4,0,45_3,15,35_4,0]_s$	0.737		
	3	$[-45_3,-15,0,45_3,15,0]_s$	0.645		

Among the results given in Table 11, the best solution is the solution designated by No. 1, which can be regarded as the global optimum solution. It is noted that if the maximum number of iterations increases, better solutions may be found. All design rules except the 10% rule have been included in the analysis. When the 10% rule applied to the analysis, no feasible solution was determined. The variations of two objective functions, together with the optimum solution points are plotted in Fig. 6 in which the solutions with zero f are highlighted by solid bullets. It is seen that after finding a solution, the process explores the search space further to find other solutions.

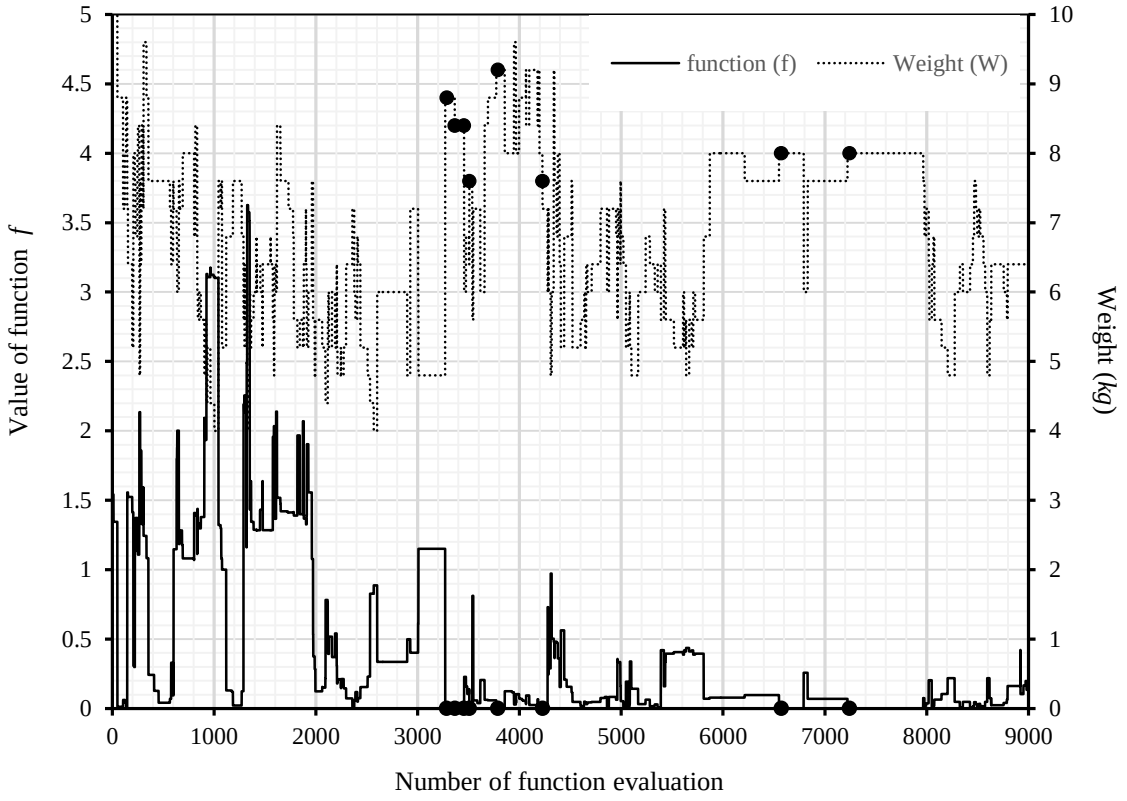

Fig. 6. Variation of objective functions with respect to the solution iteration. (Solid bullets indicates the optimum points)

7. Conclusions

An optimization procedure based on a hybrid PSO-SA method has been presented for the design of laminated composites. It has previously been shown that the hybrid PSO-SA optimization method provides good exploration and exploitation behavior, which undoubtedly is significant for solving constrained problems with narrow search spaces. Stiffness, strength, continuous layup blending, and several design rules have been included in the analysis to enhance the applicability of the results for actual engineering problems. This formulation combines all constraints into an objective function and therefore has less complexity as compared to general single-objective constrained optimization approaches. Moreover, several optimum solutions may be determined for a particular problem, which increases the flexibility of the design. Three examples, including a composite plate bending problem with layup blending constraint, have been presented to show the effectiveness of the proposed method. It can be concluded that the proposed method describes an effective and relatively simple process for the design of laminates, and it can be used as a basis for the development of an sophisticated system for design of laminates.

8. Replication of results

In this section, we provide a pseudo-code of the PSO-SA optimization method and some benchmarks for the validity of the proposed method. As stated previously in this article, the PSO-SA method is a hybrid stochastic approach that integrates the good local search of the SA within the PSO. In this regard, improvements in the global best solution will be performed by the SA method, if certain conditions were met. A new version of the SA is implemented here in which temperature reduction is adaptive [49]. In the present pseudo-code, the parameters must be set according to those given in Section 5. In Section 5, we also explained the implementation of the proposed method in solving problems in composite materials design optimization.

```
Procedure PSO-SA
n ← NumberParticles //{set initial parameters}
ω_max ← MaxLimit
ω_min ← MinLimit
i_max ← MaxIterationNumber
c_1 ← CognitiveParameter
c_2 ← SocialParameter
v_max ← UpperVelocityLimit
n_max ← SALoopLength
T_0 ← SAInitialTemperature
R_T ← SATemperatureDecrementParameter
// {generate initial state}
for i=1 to n // {initialize n particles}
   X^k ← GenerateInitialParticles
   Pb_k ← X^k
Endfor
T=T_0
// {set P_g as the best of the initial population}
Stopflag=.false.
// {determine point of best solution}
f(X^kmin ) ← min (f(X^k))
P^g ← X^kmin
for i from 1 to i_max  //{main loop}
  ω ←  ω_max-( ω_max- ω_min) ×i/ i_max
  for k from 1 to n
    R_1 ← Random(0,1)
    R_2 ← Random(0,1)
// {update velocity and position of each particle}
     v_k^(i+1) ← ωv_k^i + c_1× R_1 (Pb_k^i-X_k^i)+ c_2× R_2 (Pg^i-X_k^i)
     X_k^(i+1) ← X_k^i + v_k^(i+1)
//{check velocity for upper limit}
     If (v_k^(i+1).GE.v_max) v_k^(i+1)=v_max
     If (v_k^(i+1).LE.-v_max) v_k^(i+1)=-v_max
// {update best of each particle}
     Pb_(i+1)^k ← Pb_i^k
// {compute the global best solution of the swarm, Pg^i}
// {if  Pg^i is not improved in a PSO cycle, then send  it
//  to the modified SA procedure for an improvement}
```

```
// {Modified SA Procedure}
XSA_i ← Pg^i
    for j from 1 to n_max //{SA loop)
     XSA_c ← PickRandomState
// {compare objective function values}
      if (f(XSA_c)=< f(XSA_i) then
        XSA_i ← XSA_c  //{accept move}
         T ← T× R_T //{temperature update}
       Else
//{check for Metropolis criteria}
        R ← Random(-1,1)
        if (R<exp(-f(XSA_c)+ f(XSA_i))/T) then
          XSA_i ← XSA_c  //{accept move}
           T ← T× R_T //{temperature update}
        Endif
      Endif
//{update global best}
      Pg^i ← XSA_i
    endfor
   return // {to PSO}
// {end SA procedure}
//{check for stop criteria}
    If Stopflag=.true. then return
endfor
end
```

To verify the developed computer code and test the performance of the proposed bi-objective formulation, four mathematical constrained optimization problems have been resolved using the proposed bi-objective optimization analysis. The test functions and constraints are given in Table 12. Kim and Myung (1997) [56] described seven algorithms for mathematical constrained optimization problems based on two evolutionary programming (EP) methods. For comparison purposes, we selected two of these algorithms for each test function, which resulted in the best and the worst solutions. The obtained optimum solutions, together with the results from the literature, are summarized in Table 13. It is noticeable that the proposed bi-objective algorithm presents good results when compared with these reference values. The convergence curves are shown in Fig. 7 through Fig. 10.

Table 12
Test functions.

Function	Objective	Constraints	Bounds
F1	$100(x_2 - x_1^2)^2 + (1 - x_1)^2$	$x_1 + x_2^2 \geq 0$ $x_2 + x_1^2 \geq 0$	$-0.5 < x_1 < 0.5$ $0 < x_2 < 1$
F2	$-x_1 - x_2$	$x_2 - 2x_1^4 + 8x_1^3 - 8x_1^2 \leq 2$ $x_2 - 4x_1^4 + 32x_1^3 - 88x_1^2 + 96x_1 \leq 36$	$0 < x_1 < 3$ $0 < x_2 < 4$
F3	$0.01x_1^2 + x_2$	$x_1 x_2 - 25 \geq 0$ $x_1^2 + x_2^2 - 25 \geq 0$	$2 < x_1 < 50$ $0 < x_2 < 50$
F4	$(x_1 - 2)^2 + (x_2 - 1)^2$	$x_2 - x_1^2 \geq 0$ $x_1 + x_2 \leq 2$	----------

Table 13
Comparison of the results for mathematical constrained optimization problems.

Function	Method*	Best	Mean	Worst
F1	Algorithm #4	0.25	0.25	0.25
	Algorithm #7	0.25	0.25	0.25
	Present	0.25001	-----	-----
F2	Algorithm #1	-5.50801	-5.50801	-5.50679
	Algorithm #5	-5.50801	-5.50801	-5.50801
	Present	-5.50801	-----	-----
F3	Algorithm #2	5	5.12323	5.49622
	Algorithm #5	5	5.0002	5.00082
	Present	5	-----	-----
F4	Algorithm #3	1	1	1
	Algorithm #7	1	1	1
	Present	1	-----	-----

* The results designated by Algorithm #1 thru Algorithm#5 and Algorithm#7 were taken from Kim & Myung (1997) [56].

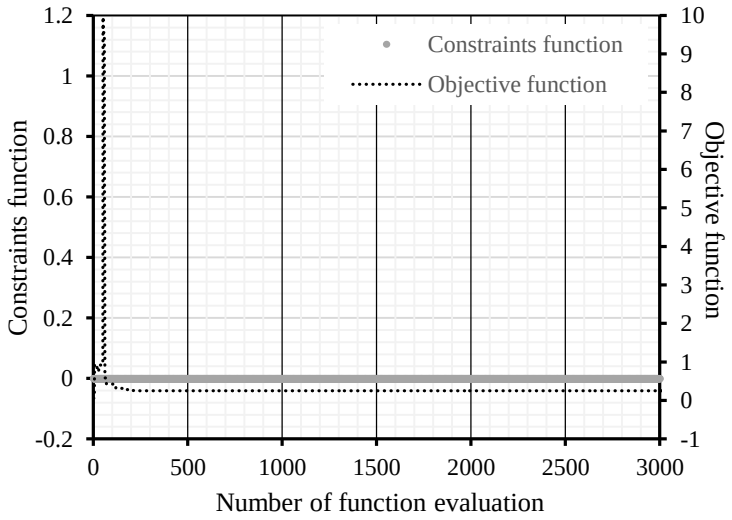

Fig. 7. Convergence curves for the function F1.

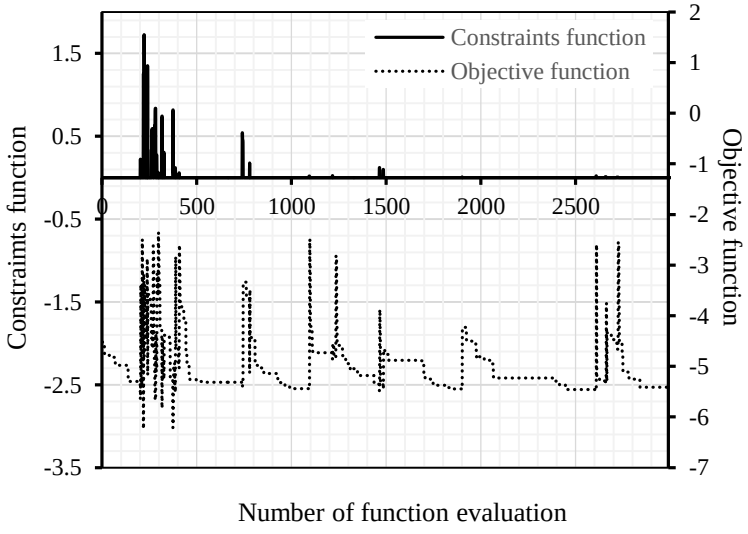

Fig. 8. Convergence curves for the function F2.

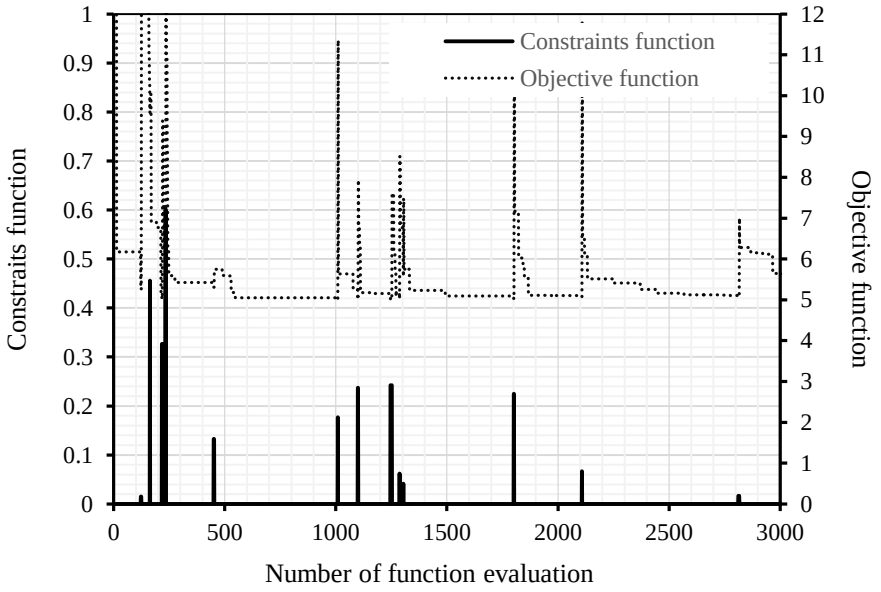

Fig. 9. Convergence curves for the function F3.

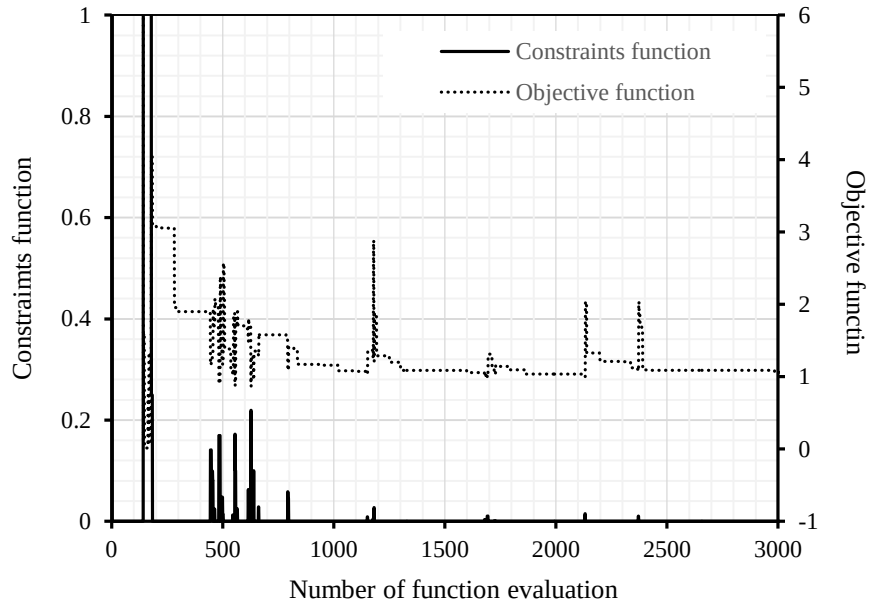

Fig. 10. Convergence curves for the function F4.

References

[1] Soutis C. Introduction: engineering requirements for aerospace composite materials. Polym. Compos. Aerosp. Ind., Elsevier; 2015, p. 1–18. doi:10.1016/B978-0-85709-523-7.00001-3.

[2] Javidrad F, Nouri R. A simulated annealing method for design of laminates with required stiffness properties. Compos Struct 2011;93:1127–35. doi:10.1016/j.compstruct.2010.10.011.

[3] Kaveh A, Dadras A, Geran Malek N. Optimum stacking sequence design of composite laminates for maximum buckling load capacity using parameter-less optimization algorithms. Eng Comput 2019;35:813–32. doi:10.1007/s00366-018-0634-2.

[4] Deveci HA, Artem HS. Optimum design of fatigue-resistant composite laminates using hybrid algorithm. Compos Struct 2017;168:178–88. doi:10.1016/j.compstruct.2017.01.064.

[5] Li X, Wang H, Li G. Reanalysis assisted metaheuristic optimization for free vibration problems of composite laminates. Compos Struct 2018;206:380–91. doi:10.1016/j.compstruct.2018.08.028.

[6] Reguera F, Cortínez VH. Optimal design of composite thin-walled beams using simulated annealing. Thin-Walled Struct 2016;104:71–81. doi:10.1016/j.tws.2016.03.001.

[7] Barbero EJ. Introduction to composite materials design. CRC press; 2017.

[8] Belardi VG, Fanelli P, Vivio F. First-order shear deformation analysis of rectilinear orthotropic composite circular plates undergoing transversal loads. Compos Part B Eng 2019;174:107015. doi:10.1016/j.compositesb.2019.107015.

[9] Adhikari B, Singh BN. An efficient higher order non-polynomial Quasi 3-D theory for dynamic responses of laminated composite plates. Compos Struct 2018;189:386–97. doi:10.1016/j.compstruct.2017.10.044.

[10] Khandan R, Noroozi S, Sewell P, Vinney J. The development of laminated composite plate theories: a review. J Mater Sci 2012;47:5901–10. doi:10.1007/s10853-012-6329-y.

[11] Guo Y, Nagy AP, Gürdal Z. A layerwise theory for laminated composites in the framework of isogeometric analysis. Compos Struct 2014;107:447–57. doi:10.1016/j.compstruct.2013.08.016.

[12] Carrera E. CZ° requirements—models for the two dimensional analysis of multilayered structures. Compos Struct 1997;37:373–83. doi:10.1016/S0263-8223(98)80005-6.

[13] Arora JS. Introduction to optimum design. (4th ed.). 707-738. Academic Press, (Chapter 18). Elsevier; 2018.

[14] Guenin B, Könemann J, Tuncel L. A gentle introduction to optimization. Cambridge University Press; 2014.

[15] An H, Chen S, Huang H. Laminate stacking sequence optimization with strength constraints using two-level approximations and adaptive genetic algorithm. Struct Multidiscip Optim 2015;51:903–18. doi:10.1007/s00158-014-1181-0.

[16] Li K, Liu X, Jin Y, Qi H, Liu X, Xu S. Structural Strength and Laminate Optimization of Composite Connecting Bracket in Manned Spacecraft Using a Genetic Algorithm. Appl Compos Mater 2019;26:591–604. doi:10.1007/s10443-018-9736-7.

[17] Wang W, Guo S, Chang N, Zhao F, Yang W. A modified ant colony algorithm for the stacking sequence optimisation of a rectangular laminate. Struct Multidiscip Optim 2010;41:711–20. doi:10.1007/s00158-009-0447-4.

[18] Zadeh PM, Fakoor M, Mohagheghi M. Bi-level optimization of laminated composite structures using particle swarm optimization algorithm. J Mech Sci Technol 2018;32:1643–52. doi:10.1007/s12206-018-0319-1.

[19] Kathiravan R, Ganguli R. Strength design of composite beam using gradient and particle swarm optimization. Compos Struct 2007;81:471–9. doi:10.1016/j.compstruct.2006.09.007.

[20] Javidrad F, Nazari M, Javidrad HR. Optimum stacking sequence design of laminates using a hybrid PSO-SA method. Compos Struct 2018;185:607–18. doi:10.1016/j.compstruct.2017.11.074.

[21] Barroso ES, Parente E, Cartaxo de Melo AM. A hybrid PSO-GA algorithm for optimization of laminated composites. Struct Multidiscip Optim 2017;55:2111–30. doi:10.1007/s00158-016-1631-y.

[22] Javidrad F, Nazari M. A new hybrid particle swarm and simulated annealing stochastic optimization method. Appl Soft Comput 2017;60:634–54. doi:10.1016/j.asoc.2017.07.023.

[23] Halpin JC. Primer on Composite Materials Analysis. Technomic Publishinf Company, Inc., USA. 1984.

[24] Sun CT, Tao QJ, Oplinger DW, J. HW. Comparative evaluation of failure analysis methods for composite laminates. In DOT/FAA/AR-95/109, Office of Aviation Research, Washington. 1996.

[25] Daniel IM. Constitutive behavior and failure criteria for composites under static and dynamic loading. Meccanica 2015;50:429–42. doi:10.1007/s11012-013-9829-1.

[26] Tsai SW, Wu EM. A General Theory of Strength for Anisotropic Materials. J Compos Mater 1971;5:58–80. doi:10.1177/002199837100500106.

[27] Kim CW, Song SR, Hwang W, Park HC, Han KS. On the failure indices of quadratic failure criteria for optimal stacking sequence design of laminated plate. Appl Compos Mater 1994;1:81–5. doi:10.1007/BF00567214.

[28] Tsai SW. Strength Characteristics of Composite Materials. . NASA CR-224, USA. 1965.

[29] Hoffman O. The Brittle Strength of Orthotropic Materials. J Compos Mater 1967;1:200–6. doi:10.1177/002199836700100210.

[30] Dong H, Wang J, Karihaloo BL. An improved Puck's failure theory for fibre-reinforced composite laminates including the in situ strength effect. Compos Sci Technol 2014;98:86–92. doi:10.1016/j.compscitech.2014.04.009.

[31] Rohwer K. Predicting fiber composite damage and failure. J Compos Mater 2015;49:2673–83. doi:10.1177/0021998314553885.

[32] Akbulut M, Sonmez FO. Design optimization of laminated composites using a new variant of simulated annealing. Comput Struct 2011;89:1712–24. doi:10.1016/j.compstruc.2011.04.007.

[33] Zhu H, Sankar B V., Marrey R V. Evaluation of Failure Criteria for Fiber Composites Using Finite Element Micromechanics. J Compos Mater 1998;32:766–82. doi:10.1177/002199839803200804.

[34] Bailie JA, Ley RP, Pasricha A. A summary and review of composite laminate design guidelines. NASA contract final report NAS1-19347, National Aeronautics and Space Administration, Langley Research Center, USA. 1997.

[35] Kim J-S, Kim N-P, Han S-H. Optimal stiffness design of composite laminates for a train carbody by an expert system and enumeration method. Compos Struct 2005;68:147–56. doi:10.1016/j.compstruct.2004.03.009.

[36] Vannucci P, Verchery G. A special class of uncoupled and quasi-homogeneous laminates. Compos Sci Technol 2001;61:1465–73. doi:10.1016/S0266-3538(01)00039-2.

[37] Montemurro M. An extension of the polar method to the First-order Shear Deformation Theory of laminates. Compos Struct 2015;127:328–39. doi:10.1016/j.compstruct.2015.03.025.

[38] Middleton TH. Composite Materials in Aircraft Structures. John Wiley and Sons. 1990.

[39] Niu MC-Y. Composite Airframe Structures, Third edition. Hong Kong Conmilit Press Ltd. 2010.

[40] Todoroki A, Sasada N, Miki M. Object-Oriented Approach to Optimize Composite Laminated Plate Stiffness with Discrete Ply Angles. J Compos Mater 1996;30:1020–41. doi:10.1177/002199839603000904.

[41] Wang D, Tan D, Liu L. Particle swarm optimization algorithm: an overview. Soft Comput 2018;22:387–408. doi:10.1007/s00500-016-2474-6.

[42] Kennedy J, Eberhart R. Particle swarm optimization. Proc. IEEE Int. Conf. Neural Netw. IV, 1942–1948., vol. 4, IEEE; 1995, p. 1942–8. doi:10.1109/ICNN.1995.488968.

[43] Taherkhani M, Safabakhsh R. A novel stability-based adaptive inertia weight for particle swarm optimization. Appl Soft Comput 2016;38:281–95. doi:10.1016/j.asoc.2015.10.004.

[44] Schneider JJ, Puchta M. Investigation of acceptance simulated annealing — A simplified approach to adaptive cooling schedules. Phys A Stat Mech Its Appl 2010;389:5822–31. doi:10.1016/j.physa.2010.08.045.

[45] Atiqullah MM. An Efficient Simple Cooling Schedule for Simulated Annealing, 2004, p. 396–404. doi:10.1007/978-3-540-24767-8_41.

[46] Xia W, Wu Z. A hybrid particle swarm optimization approach for the job-shop scheduling problem. Int J Adv Manuf Technol 2006;29:360–6. doi:10.1007/s00170-005-2513-4.

[47] Xi-Huai Wang, Jun-Jun Li. Hybrid particle swarm optimization with simulated annealing. Proc. 2004 Int. Conf. Mach. Learn. Cybern. (IEEE Cat. No.04EX826), vol. 4, IEEE; n.d., p. 2402–5. doi:10.1109/ICMLC.2004.1382205.

[48] Shieh H-L, Kuo C-C, Chiang C-M. Modified particle swarm optimization algorithm with simulated annealing behavior and its numerical verification. Appl Math Comput 2011;218:4365–83. doi:10.1016/j.amc.2011.10.012.

[49] Javidrad F, Nazari M, Javidrad HR. A variable Markov chain length strategy for improving simulated annealing convergence behavior: An experimental verification. In A. Scollen & T. Hargraves (Eds.), Simulated Annealing, Introduction, Applications and Theory n.d.:221–68.

[50] Grosset L, LeRiche R, Haftka RT. A double-distribution statistical algorithm for composite laminate optimization. Struct Multidiscip Optim 2006;31:49–59. doi:10.1007/s00158-005-0551-z.

[51] Venter G, Haftka RT. Constrained particle swarm optimization using a bi-objective formulation. Struct Multidiscip Optim 2010;40:65–76. doi:10.1007/s00158-009-0380-6.

[52] Kristinsdottir BP, Zabinsky ZB, Tuttle ME, Neogi S. Optimal design of large composite panels with varying loads. Compos Struct 2001;51:93–102. doi:10.1016/S0263-8223(00)00128-8.

[53] Liu D, Toroporov V V., Querin OM, Barton DC. Bilevel Optimization of Blended Composite Wing Panels. J Aircr 2011;48:107–18. doi:10.2514/1.C000261.

[54] Adams DB, Watson LT, Gürdal Z, Anderson-Cook CM. Genetic algorithm optimization and blending of composite laminates by locally reducing laminate thickness. Adv Eng Softw 2004;35:35–43. doi:10.1016/j.advengsoft.2003.09.001.

[55] Irisarri F-X, Lasseigne A, Leroy F-H, Le Riche R. Optimal design of laminated composite structures with ply drops using stacking sequence tables. Compos Struct 2014;107:559–69. doi:10.1016/j.compstruct.2013.08.030.

[56] Jong-Hwan Kim, Hyun Myung. Evolutionary programming techniques for constrained optimization problems. IEEE Trans Evol Comput 1997;1:129–40. doi:10.1109/4235.687880.